Alexandria Engineering Journal (2016) 55, 2821–2832

HOSTED BY

Alexandria University

Alexandria Engineering Journal

www.elsevier.com/locate/aej
www.sciencedirect.com

ORIGINAL ARTICLE

Seismic energy dissipation study of linear fluid viscous dampers in steel structure design

A. Ras *, N. Boumechra

Civil Engineering Department, Faculty of Technology, University of Tlemcen, BP 230, Tlemcen 13000, Algeria

Received 3 May 2014; revised 3 July 2016; accepted 11 July 2016
Available online 27 July 2016

KEYWORDS

Structure;
Bracing;
Energy dissipation;
Viscous fluid damper;
Fast nonlinear analysis (FNA);
Seismic analysis

Abstract Energy dissipation systems in civil engineering structures are sought when it comes to removing unwanted energy such as earthquake and wind. Among these systems, there is combination of structural steel frames with passive energy dissipation provided by Fluid Viscous Dampers (FVD). This device is increasingly used to provide better seismic protection for existing as well as new buildings and bridges. A 3D numerical investigation is done considering the seismic response of a twelve-storey steel building moment frame with diagonal FVD that have linear force versus velocity behaviour. Nonlinear time history, which is being calculated by Fast nonlinear analysis (FNA), of Boumerdes earthquake (Algeria, May 2003) is considered for the analysis and carried out using the SAP2000 software and comparisons between unbraced, braced and damped structure are shown in a tabulated and graphical format. The results of the various systems are studied to compare the structural response with and without this device of the energy dissipation thus obtained. The conclusions showed the formidable potential of the FVD to improve the dissipative capacities of the structure without increasing its rigidity. It is contributing significantly to reduce the quantity of steel necessary for its general stability.

1. Introduction

Man has always lived with earthquakes. Some of them are so small that they are not felt; others are so strong that they can destroy an entire city, cause major damage to infrastructures (bridges, buildings, etc.) and kill thousands of people.

During a seismic event, the input energy from the ground acceleration is transformed into both kinetic and potential (strain) energy which must be either absorbed or dissipated through heat. However, for strong earthquakes a large portion of the input energy will be absorbed by hysteretic action (damage to structure). So for many engineers, the most conventional approach to protect the structures (buildings and bridges) against the effects of earthquakes is to increase the stiffness. This approach is not always effective, especially when it is an environment that promotes resonance and amplification of seismic forces.

To do this, the field of the earthquake engineering has made significant inroads catalysed by the development of computational techniques on computer and the use of powerful testing facilities. This has favoured the emergence of several innovative technologies such as the introduction of special damping

* Corresponding author at: EOLE, Department of Civil Engineering, University of Tlemcen, BP 230, Tlemcen, Algeria.
E-mail address: ouahab_ras@yahoo.fr (A. Ras).
Peer review under responsibility of Faculty of Engineering, Alexandria University.

http://dx.doi.org/10.1016/j.aej.2016.07.012

devices in the structures, which have the immediate effect of increasing the critical damping ratio right up 20–30% (against 5% value usually used for metal structures) and at the same time reducing the stresses and strains generated by earthquakes. This approach, is commonly known as the "energy dissipation", and has the capacity to absorb significant efforts without damaging the structure and ensuring the protection of human lives and property [1].

This approach of seismic energy dissipation is made clear by considering the following time-dependent conservation of energy relationship [2]:

$$E(t) = E_k(t) + E_s(t) + E_h(t) + E_d(t) \quad (1)$$

where

E is the absolute energy input from the earthquake motion;
E_k is the absolute kinetic energy;
E_s is the elastic (recoverable) strain energy, and E_h is the irrecoverable energy dissipated by the structural system through inelastic or other forms of action (viscous and hysteretic);
E_d is the energy dissipated by the supplemental damping system and t represents time.

The absolute input energy, E, represents the work done by the total base shear force at the foundation on the ground displacement and thus accounts for the effect of the inertia forces on the structure.

In the conventional design approach, the term E_d in Eq. (1) is equal to zero. In this case acceptable structural performance is accomplished by the occurrence of inelastic deformations, which has direct effect of increasing E_h. Finally the increased flexibility acts as filter which reflects a portion of seismic energy.

Introduction of supplemental damping devices in the structure involves increasing the term E_d in Eq. (1) and accounts for the major seismic energy that is absorbed during the earthquake [6].

In a supplemental dissipation energy system, mechanical devices are incorporated in the frame of the structure or within the base isolation system (Fig. 1).

Among these devices, there are the Fluid Viscous Dampers (FVD) which are included in the passive control systems of structural response. These systems have the ability to transmit developed forces according to the request of the structural response. Passive control devices dissipate energy in the structure, but cannot increase it. Because of their great ability to return a building to its original position after an earthquake, they are increasingly used in the bracing structures in civil engineering in general and in the metallic high-rise structures in particular. The additional cost of the damper is typically offset by the savings in the steel weight and foundation concrete volume [3]. This device and its effect on the seismic structure response are the subject of this study.

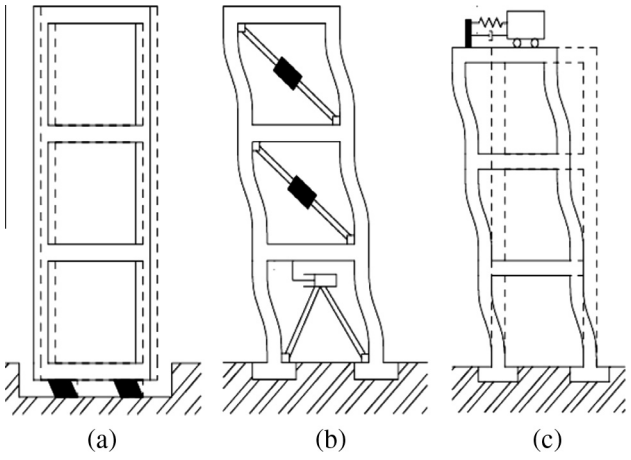

Figure 1 Passive response control system: (a) Seismic isolation, (b) FVD, (c) dynamic vibration absorber [4].

2. Fluid viscous damper

Fluid viscous dampers were initially used in the military and aerospace industry. They were designed for use in structural engineering in the late of 1980s and early of 1990s. FVD typically consist of a piston head with orifices contained in a cylinder filled with a highly viscous fluid, usually a compound of silicone or a similar type of oil. Energy is dissipated in the damper by fluid orifice when the piston head moves through the fluid [5]. The fluid in the cylinder is nearly incompressible, and when the damper is subjected to a compressive force, the fluid volume inside the cylinder is decreased as a result of the piston rod area movement. A decrease in volume results in a restoring force. This undesirable force is prevented by using an accumulator. An accumulator works by collecting the volume of fluid that is displaced by the piston rod and storing it in the makeup area. As the rod retreats, a vacuum that has been created will draw the fluid out. A damper with an accumulator is illustrated in Fig. 2 [6].

2.1. Characteristics of fluid viscous dampers

FVD are characterised by a resistance force F. It depends on the velocity of movement, the fluid viscosity and the orifices size of the piston. The value of P is given by the relationship [7]:

$$P = C_d \cdot \left(u_d^{\bullet}\right)^{\alpha} \cdot \sin\left(u_d^{\bullet}\right) \quad (2)$$

with

$$u_d(t) = u_0 \cdot \sin(\omega \cdot t) \quad (3)$$

where

$u_d^{\bullet}$ is the velocity between two ends of the damper;
C_d is the damping constant;
u_0 is the amplitude of the displacement, ω is the loading frequency, and t is time;
α is an exponent which depends on the viscosity properties of the fluid and the piston.

The value of the constant α may be less than or equal to 1. Figs. 3 and 4 show the force velocity and the force displacement relationships for three different types of FVD. They characterise the behaviour of the viscous damper. With $\alpha = 1$ the device is called linear viscous damper and for $\alpha < 1$ non-linear FVD which is effective in minimising high velocity shocks. Damper with $\alpha > 1$ has not been seen often in practical application. The non-linear damper can give a larger damping force than the two other types (Fig. 3) [8].

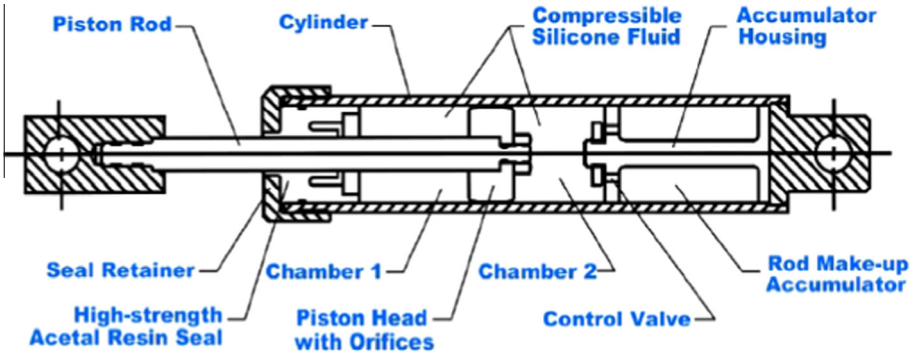

Figure 2 Fluid viscous dampers (FVD).

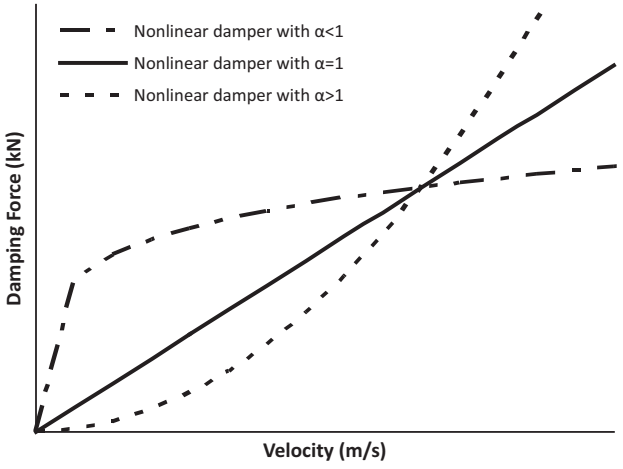

Figure 3 Force velocity relationship of FVD.

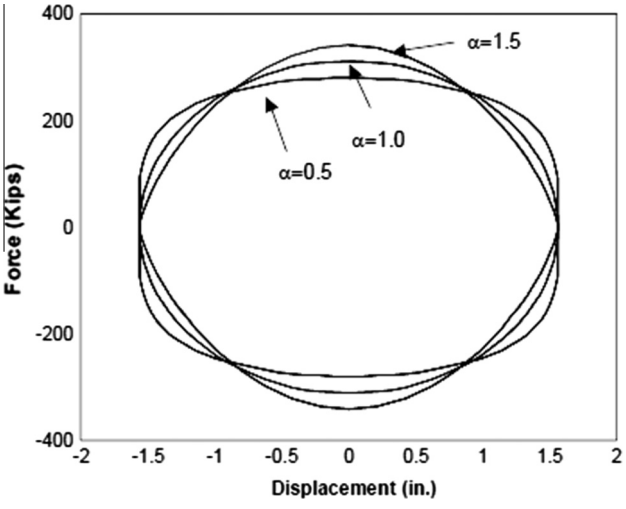

Figure 4 Force displacement relationship of FVD.

Fig. 4 shows that the plot has different shapes for the different values of α. At the frequency of loading used to create the loops enclosed areas for the different damper are all equal, but the values of the damping coefficient are all different.

The resisting force in the FVD, P, can be described by the following equation:

$$P = K_1 \cdot u_d + C_d \cdot \frac{du_d}{dt} \tag{4}$$

where K_1 is the storage stiffness and C is the damping coefficient given by

$$C_d = \frac{K_2}{\omega} \tag{5}$$

where K_2 is the loss stiffness. In Eq. (4) the first term represents the force due to the stiffness of the damper, which is in phase with the motion, and the second term represents the force due to the viscosity of the damper, which is 90° out of phase with the motion. Fig. 5a plots the force-displacement relationship for the first and second terms of Eq. (4), while (c) plots the total force. Fig. 5b shows the structure's behaviour without dampers.

FVD allow very significant energy dissipation where the stress-strains diagram shows a hysteretic loop approaching an ellipse for a pure viscous linear behaviour. The absence of storage stiffness makes the natural frequency of the structure incorporated with the damper remains the same. This advantage will simplify the design procedure with supplemental viscous devices. However if the damper develops restoring force the loop will be changed in Fig. 5a–c. It turns from viscous behaviour to viscoelastic behaviour. The maximum energy amount that this type of damper can dissipate in a very short time is only limited by the thermal capacity of lead and steel tube.

2.2. Analytical model of the fluid viscous damper

Fluid viscous dampers exhibit a viscoelastic behaviour, which can be best predicted with the Kelvin and Maxwell models for linear and non linear models respectively (Fig. 6) [10].

The model can also be described by the following equation:

$$P(t) + \lambda \frac{dP(t)}{dt} = C_d \cdot \frac{du_d}{dt} \tag{6}$$

where $u_d(t) = u_0 \cdot \sin(\omega t)$. P is the damper output force, λ is the relaxation time, C_d is the damping constant at zero frequency, and u is the displacement of the piston head with respect to the damper housing. The relaxation time for the damper is defined as

$$\lambda = \frac{C_d}{K_1} \tag{7}$$

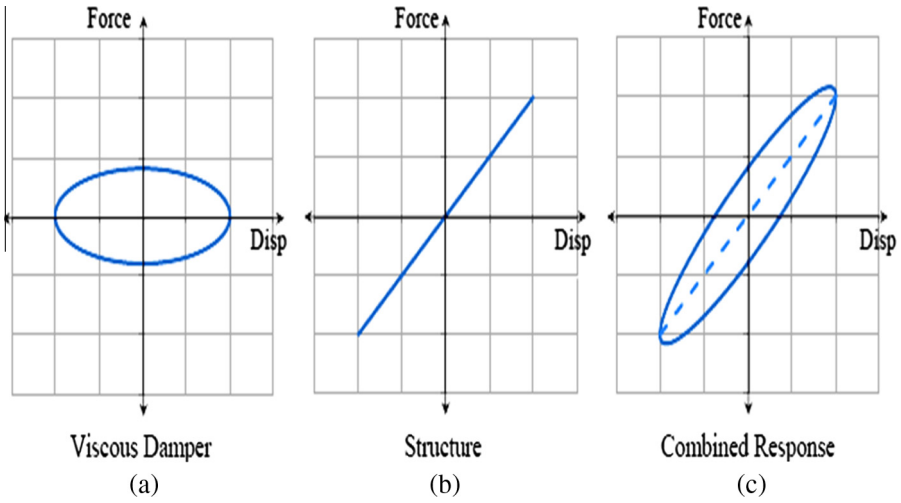

Figure 5 Hysteretic curve of FVD [9].

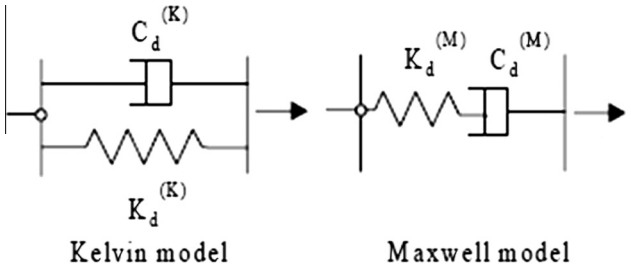

Figure 6 Maxwell model.

where K_1 is the storage stiffness of the damper at infinite frequency.

For identification of the damper behaviour, the classical Maxwell model of Eq. (6) was generalised to the following form in which the derivatives are of fractional order [11]:

$$P(t) + \lambda \cdot D^r[P(t)] = C_d \cdot D^q[u(t)] \tag{8}$$

where $D^r[P(t)]$ and $D^q[u(t)]$ are fractional derivatives of orders r and q, which are based on material properties. For complex viscoelastic behaviour, the fractional derivative model typically offers an approved ability to describe the damper behaviour over a wide frequency range. Other more advanced models of viscoelasticity have been examined for modelling the behaviour of fluid damper. For example Makris et al. [12] examined an even more advanced model of viscoelasticity to study the behaviour of fluid dampers. In this model the order of the time derivatives and the coefficients are complex-valued. The resulting models may be regarded as simplified forms of linear models of viscoelasticity.

2.2.1. Linear fluid viscous damper

The current study focused on linear fluid viscous damping. The model described by Eq. (8) can be simplified to obtain a more useful model of linear viscous damping. When $r = q = 1$ the model becomes the Maxwell model described by Eq. (6). The device parameters, λ and C_d, were obtained from experimental tests performed in studies by Constantinou and Symans [13]. If the frequency of vibration is below the cut-off frequency, the second term in Eq. (8) drops out and the model of the damper can be simplified as

$$P(t) = C_d \cdot \frac{du_d}{dt} \tag{9}$$

where C_d is independent of the frequency, but dependent on ambient temperature.

The energy dissipated by damper is [14]

$$W_D = \oint F_D \cdot du \tag{10}$$

$$\Rightarrow W_D = \oint C_d \cdot u^{\bullet} \cdot du = \int_0^{2\cdot\pi/\omega} C_d \cdot u^{\bullet 2} \cdot dt$$

$$\Rightarrow W_D = C_d \cdot u_0^2 \cdot \omega^2 \int_0^{2\cdot\pi} C_d \cdot \cos^2(\omega \cdot t) \cdot d(\omega t)$$

$$\Rightarrow W_D = \pi \cdot C_d \cdot u_0^2 \cdot \omega \tag{11}$$

Recognising that the damping ratio contributed by the damper can be expressed as $\xi_d = C_d/C_{cr}$ is obtained and natural excitation frequency is

$$\omega_0 = 2 \cdot \pi/T = \sqrt{K/M}$$

$$\Rightarrow W_D = \pi \cdot C_d \cdot u_0^2 \cdot \omega = \pi \cdot \xi_d \cdot C_{cr} \cdot u_0^2 \cdot \omega$$

$$\Rightarrow W_D = 2 \cdot \pi \cdot \xi_d \cdot \sqrt{K \cdot M} \cdot u_0^2 \cdot \omega$$

$$\Rightarrow W_D = 2 \cdot \pi \cdot \xi_d \cdot K \cdot u_0^2 \cdot \frac{\omega}{\omega_0}$$

$$\Rightarrow W_D = 4 \cdot \pi \cdot \xi_d \cdot W_s \cdot \frac{\omega}{\omega_0} \tag{12}$$

where C_{cr}, K, M, ω_0 and $W_s = K \cdot u_0^2/2$ are respectively the critical damping coefficient, stiffness, mass, natural frequency and elastic strain energy of the system. The damping ratio attributed to the damper can then be expressed as

$$\xi_d = \frac{W_D \cdot \omega_0}{4 \cdot \pi \cdot W_s \cdot \omega} \tag{13}$$

W_D and W_s are illustrated in Fig. 7. Under earthquake excitation, ω is essentially equal to ω_0 and Eq. (13) is reduced to

$$\xi_d = \frac{W_D}{4 \cdot \pi \cdot W_s} \tag{14}$$

2.3. Modelling of system with fluid viscous damper

Fig. 8 shows a structure with a multi degree of freedom connected to FVD. The motion equation of the structure subjected to a ground vibration becomes [4]

$$[M] \cdot U^{\bullet\bullet} + [(C)] \cdot U^{\bullet} + [(K)] \cdot U + F_d(t) = -[M] \cdot x_g^{\bullet\bullet} \tag{15}$$

where

M: Structure mass,
K = Structure equivalent stiffness,
C: Damping coefficient of the structure,
$F_d(t)$: FVD force vector,
$U, U^{\bullet}, U^{\bullet\bullet}$: Displacement, velocity and acceleration vectors of the structure,
$x_g^{\bullet\bullet}$: Ground acceleration (Earthquake).

Considering a MDOF system as shown in Fig. 9 the total effective damping ratio of the system ξ_{eff}, is defined as

$$\xi_{eff} = \xi_0 + \xi_d \tag{16}$$

where ξ_0 is the inherent damping ratio of the MDOF without dampers, and ξ_d is the damping ratio of the FVD. Extended from the concept of SDOF system, Eq. (17) is used by FEMA273 (Federal Emergency Management Agency) [15] to represent ξ_d.

$$\xi_d = \frac{\sum W_j}{4 \cdot \pi \cdot W_K} \tag{17}$$

$\sum W_j$ is the sum of the energy dissipated by the jth damper of the system in one cycle; W_K is the elastic strain energy of the frame. W_K is equal to $\sum F_i \cdot U_i$ where F_i is the storey shear and U_i is the storey drift of the ith floor. Now the energy dissipated by the FVD can be expressed by

$$\sum_j W_j = \sum_j \pi \cdot C_j \cdot u_j^2 \cdot \omega_0 = \frac{2 \cdot \pi^2}{T} \cdot \sum_j C_j \cdot u_j^2 \tag{18}$$

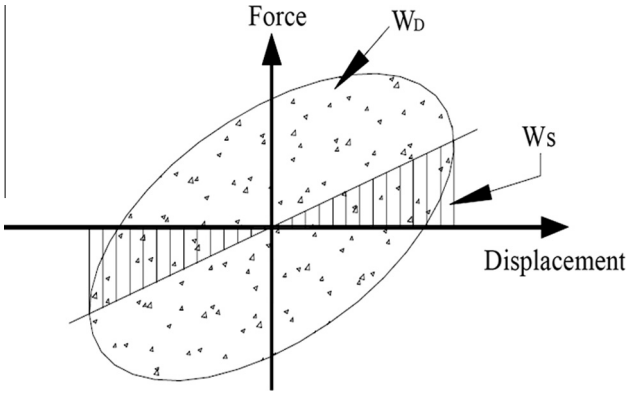

Figure 7 Definition of dissipation energy W_D and elastic strain energy of SDOF with FVD.

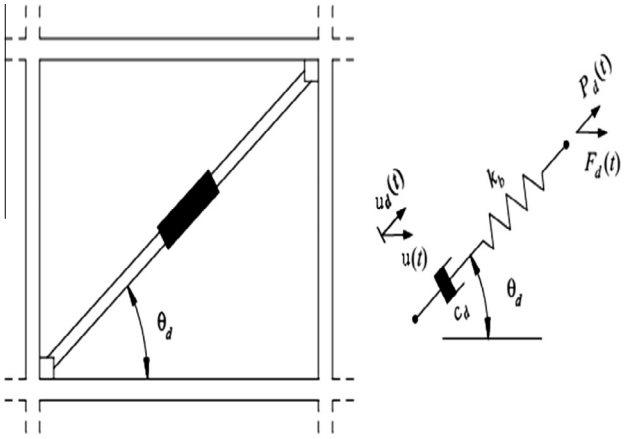

Figure 8 Multiple degree of freedom (MDOF) structure with FVD.

where u_j is the relative axial displacement between two ends of the damper.

Usually, only the first mode of the MDOF system is considered in the simplified procedure of practical applications. Using the modal strain energy method, the energy dissipated by dampers and elastic strain energy provided by the structure without FVD can be rewritten as

$$\sum_j W_j = \frac{2 \cdot \pi^2}{T} \cdot \sum_j C_j \cdot \phi_{rj}^2 \cdot \cos^2 \theta_j \tag{19}$$

$$\text{and :} \quad W_K = \frac{1}{2} \cdot \Phi_1^T \cdot [K] \Phi_1 = \frac{1}{2} \cdot \Phi_1^T \cdot \omega^2 \cdot [M] \Phi_1$$

$$W_K = \frac{1}{2} \cdot \sum_i \omega^2 \cdot M_i \cdot \phi_i^2 = \frac{2 \cdot \pi^2}{T^2} \cdot \sum_i M_i \cdot \phi_i^2 \tag{20}$$

where $[K]$, $[M]$ and Φ_1 are respectively, stiffness matrix, mass matrix and first mode shape of system; ϕ_{rj} is the relative horizontal displacement of damper j corresponding to first mode shape. ϕ_i is the first mode shape at floor and θ_j is the inclined angle of the damper j. Substituting Eqs. (17), (19) and (20) into (16), the ξ_{eff} of a structure with linear FVD is given by

$$\xi_{eff} = \xi_0 + \frac{T \cdot \sum_j C_j \cdot \phi_{rj}^2 \cdot \cos^2 \theta_j}{4 \cdot \pi \cdot \sum_i M_i \cdot \phi_i^2} \tag{21}$$

Corresponding to a desired added damping ratio, there is no substantial procedure suggested by the design codes for distributing C values over the whole buildings. When designing the dampers, it may be convenient to distribute C values equally in each floor. However, many experimental results have shown that the efficiency of damper on the upper stories is smaller than the lower ones [16], Yang et al. [17] conducted a series of experiments with different numbers and configurations of the dampers. They used a five-storey and a six-storey steel frame building. They found that the use of more dampers does not necessarily result in a better vibration reduction, etc. Hence an efficient distribution of the C values of the dampers may be to size the horizontal damper force in

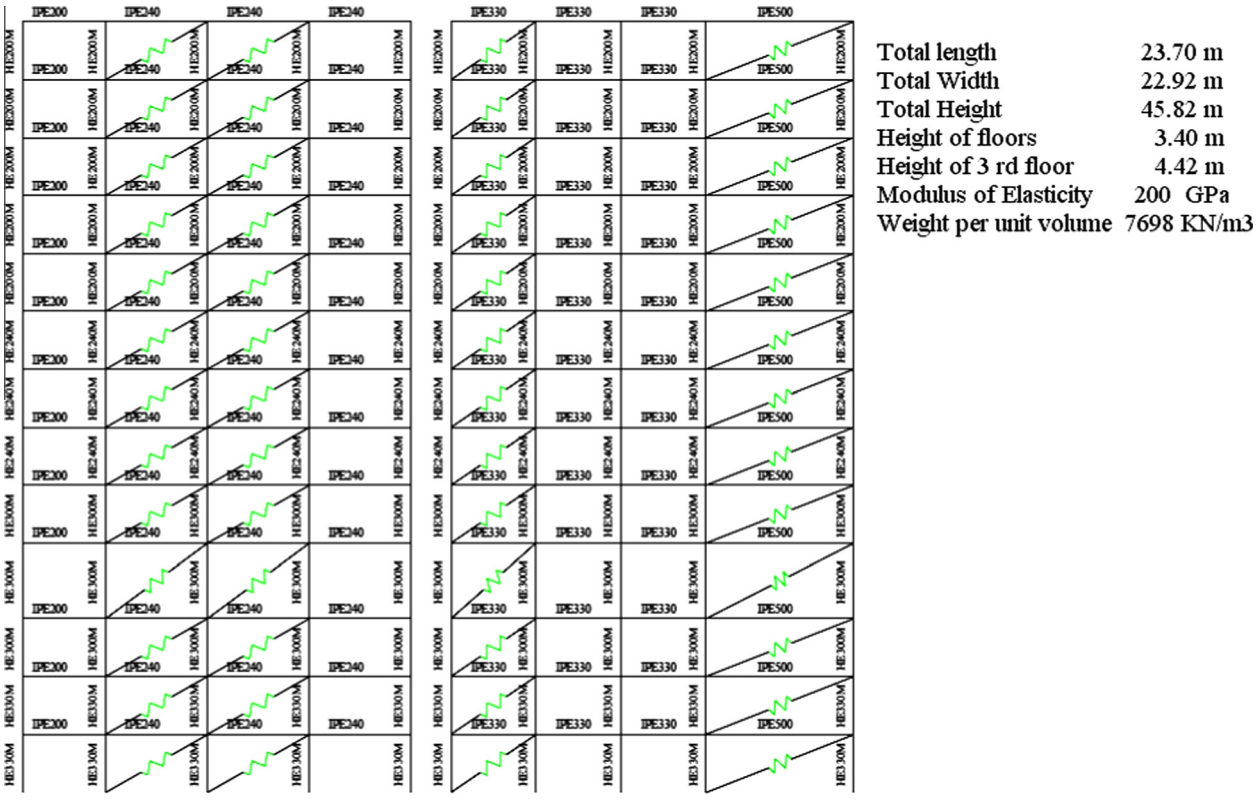

Figure 9 Modelling of twelve-storey building connected to FVD.

proportion of the storey shear forces of the structure without braces.

3. Case study

3.1. Structure characteristics

A twelve-storey steel building modelled as 3D moment resisting frame is analysed with and without viscous dampers using SAP2000 [18]. The profiles of the various frame elements and properties of the building are shown in Fig. 9.

The damper stiffness inserted into the SAP2000 model is equal to one diagonal of L120x13 profile.

The lateral dynamic load applied to the structure was simulated by nonlinear time history (FNA) of the Boumerdes earthquake (Algeria May 2003). This is given in the form of text file having 7000 points of acceleration data equally spaced at 0.05 s. The time history data of the aforementioned ground motion are illustrated in Fig. 10. The use of Nonlinear time history (NLTH) analysis is mandated for most passively damped structures because the earthquake vibration of most civil engineering structure will induce deformation in one or more structural element beyond their yield limit. Therefore, the structure will respond to a nonlinear relationship between force and deformation. The results are summarised in the following paragraph.

Fig. 11 shows the response spectra of the time histories of the frame with $\xi_{eff} = 5\%$ (no dampers) in comparison with the Design Earthquake Spectra from the building from the RPA/2003 (Algerian seismic code) [19].

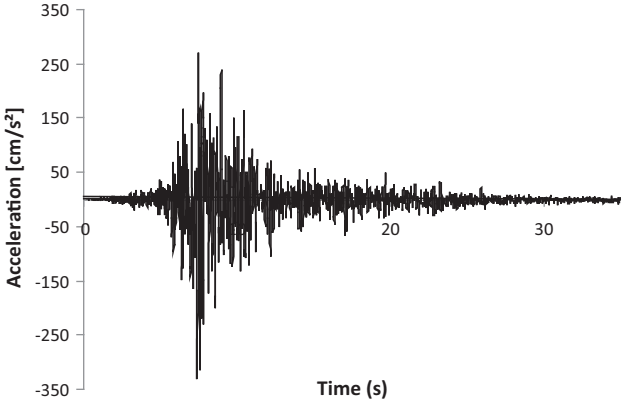

Figure 10 Boumerdes ground acceleration (north-west).

3.2. Results and interpretation

To maximise the performance of dampers, upstream optimisation study on the location of diagonal steel bracing element (cross brace with L120x13 angle profile) positions was conducted on twelve alternatives (Fig 12).

The results show that the alternative No. 10 was the best in vibration's period and mass participation. It was compared with non-braced and damped models. The results are summarised in Table 1. Note that the condition of 90% of mass participation (M.P.) required by RPA99/2003 (Algerian seismic code) [19], has been satisfied in the case of the braced alternative at the mode no. 8.

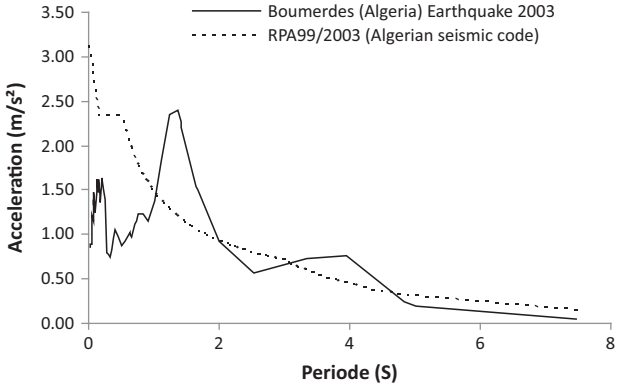

Figure 11 Comparisons of damped acceleration response spectra for selected time histories with design spectra from the RPA99/2003.

All damping coefficients C_d of the dampers added to the structure have equal values according to research results [17] which indicate that it is reasonable to assume that all damping coefficients C_d may be equal.

As expected, the fundamental period of vibration for the braced structure decreases due to the increased stiffness. In the third case, the period decreases due to the added stiffness resulting from the use of dampers. It should be noted that the number of diagonals used in the third case is reduced by half compared to the second case; however, the values of the periods remain close.

The time history analysis response in terms of displacement and acceleration at top of the structure in three models (Fig. 13) shows significant reduction in the structure equipped with FVD in comparison with unbraced structure ($\xi_{eff} = 5\%$). When the top displacement value of the unbraced structure reaches maximum, the corresponding one of the damped structure ($\xi_{eff} = 35\%$) decreases by 30%.

It also can be observed that the acceleration response of the two cases, damped and self-supporting is almost the same. It means that the increase of structure stiffness with the addition of the supplement dampers does not increase its acceleration; unlike the comparison with cross braces case where the model of the FVD response decreases at the peak by 37%.

This can lead to reduce the unpleasant effects of acceleration for occupants of these structures but also for non-structural parts, pipes, false ceilings, etc.

Table 1 Results of comparison of the three models.

Unbraced structure		Braced structure (cross)		FVD Damped structure (FVD)	
Period (s)	M.P. (%)	Period (s)	M.P. (%)	Period (s)	M.P. (%)
$T_1 = 7.47$	76.36	$T_1 = 2.02$	73.13	$T_1 = 2.32$	77.87
$T_2 = 4.84$	75.50	$T_2 = 1.87$	76.21	$T_2 = 2.31$	75.00
$T_3 = 3.95$	76.13	$T_3 = 1.33$	77.77	$T_3 = 1.67$	74.65

The verification of structural members' stability is checked in combinations including earthquake (RPA99-2003 section 5.2); however, a time history analysis of the top axial (N), shear (V) forces and moment (M) of the seismic loading has been carried out (Fig 14) [20]. The results showed decrease values for reinforced cross brace and FVD models with a net benefit to the dissipative device model. This decrease is due to the additional stiffness provided by the reinforcing elements but it is also due to the increase of damping ratio for the FVD model. It is also important to note that in the braced structure, the cross diagonals transmit a very significant axial force to its near columns, valued at 5 times the ones of the damped model. This last has the ability to decrease them by developing resisting forces induced by the dampers.

Fig. 15 shows the ability of FVD to reduce the base shear force. Note that it becomes very important in the cross braced case. It is due to the decrease of the fundamental period ($T = 2.02$ s) which makes greater acceleration but these forces decrease rapidly over time due to the stiffness of the system. Unlike the unbraced model where the base shear force is not very important ($T = 7.47$ s) but remains constant throughout the duration of the signal, in the third model, forces are low ($T = 2.32$ s) and they disappear quickly and completely after 15 s of vibration. This is due to the capacity of FVD to produce a passive control system by balancing quickly the load forces to the resistance and damping forces.

Fig. 16 illustrates the variation of the axial force (N), the shear force and the bending moment according to the FVD damping constant C_d, for X and Y directions of earthquake.

The curves have shown an exponential pace that can be compared to two straight lines. The first line shows a decreasing force versus an increase of damping constant until the intersection with the second line where the values become

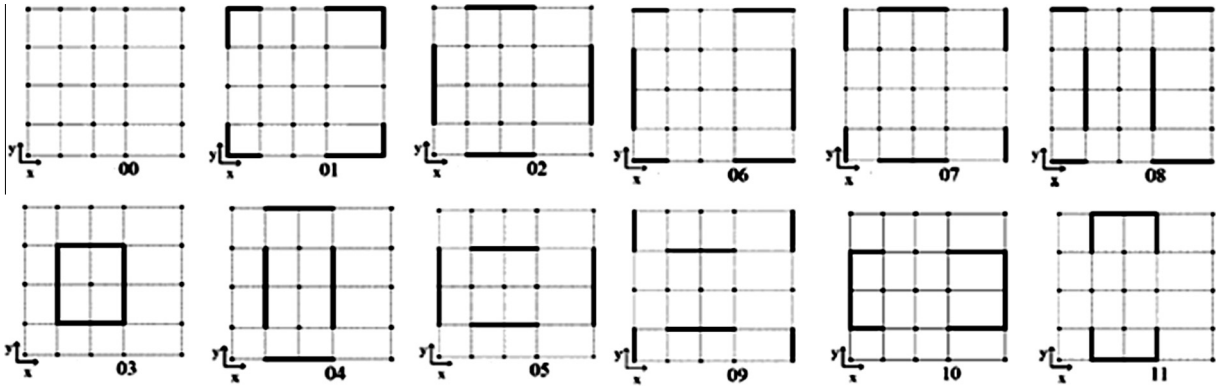

Figure 12 The twelve alternatives of diagonal location.

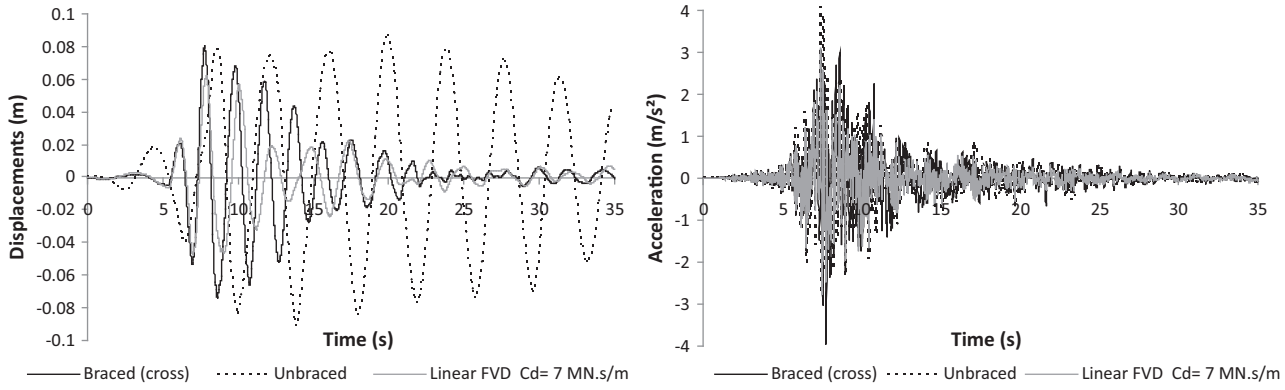

Figure 13 Time history displacement and acceleration response.

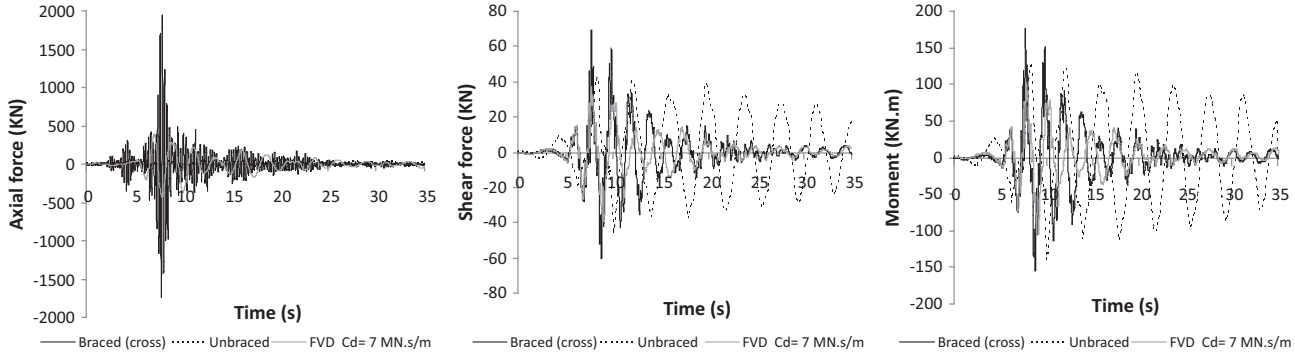

Figure 14 Time history variation of N, T and M.

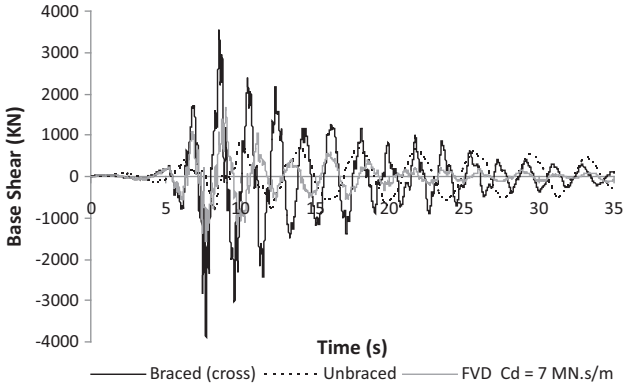

Figure 15 Time history variation of base shear force.

almost constant. We can conclude that for $C_d = 25$ MN s/m the damped structure, can fully absorb the input energy of the seismic signal and supplement damping will not affect the system which will be already completely dissipated. This conclusion was confirmed by the results summarised in Table 2 which shows the variation of the FVD damping ratio ξ_d according to its damping coefficient C_d. It may be seen in Table 2 that the increase of C_d generates an augmentation of the damping capacity of the structure to resist to the seismic, up to a value of $\xi_d = 100\%$. This last result represents only a theoretical value since in practice, the fluid viscous damper at this ratio dissipates the input energy in the form of heat which can cause an increase in the heat causing degradation in its good functioning.

The results shown above are in accordance with those found by Lin and Chen [21] who conducted experiments on shaking table to verify the numerical model computed by sap 2000.

In the curves of Fig. 17 the variation of the input and the damping energies of the system were compared for the cases of frame (Fig. 17a) and damped structures ($C_d = 7$ MN s/m) (Fig. 17b). They show that an addition of supplemental dampers results an increase of the absolute input energy. This is not surprising since at the end of the earthquake the absolute input energy must be equal to the dissipated energy in the system (Fig. 17b). Therefore, it is expected that the structure with dampers ($\xi_{eff} = 35\%$) would have a large absolute input energy at the end of the earthquake. The input energy at time t is the integral of the base shear over the ground displacement and it is described in the following equation:

$$E(t) = \int_0^t m \cdot \left[u^{\bullet\bullet}(t) + u_g^{\bullet\bullet}(t)\right] \cdot du_g(t) \tag{22}$$

So as mentioned above the increase of stiffness in the structure increases relatively the base shear in the damped model and consequently develops its input energy. In contrast, the undamped structure with its relatively low inherent damping ($\xi_{eff} = 5\%$) has low ability to dissipate load energy which results in a small absolute input energy at the end of earthquake. These results are comparable to those achieved by other works [6]. However the energy of the seismic signal is

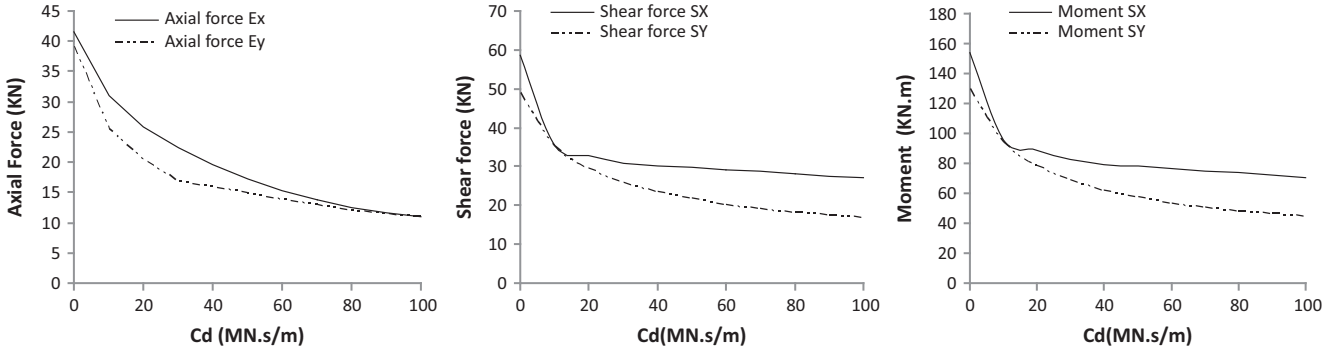

Figure 16 Variations of N, T and M versus damping constant.

Table 2 Variation of ξ_d according to C_d.

C_d (MN s/m)	W_s (J)	W_D (J)	ξ_d (%)
0	168.63	0	0
0.5	149.58	28.4	3
2	119.74	75.63	10
4	98	113.63	18.46
7	78.31	150.82	30.5
10	65.7	176.06	42.67
15	52.14	204.33	62.5
20	43.44	223.31	81.6
25	37.37	237.14	100

completely dissipated by the addition of the modal damping (W_s) and link damping (W_D) energies. It means that the reduction in ductility demand is facilitated through displacement reductions that come with increased damping.

The analyses of the FVD damped structure are run with a range of different damping ratios. The plot of Fig. 18 shows the hysteric loops of the dampers (placed at 7th storey of a building) response contributing with no supplemental damping ($\xi_d = 0\%$) (Fig. 18a), 30% damping ($\xi_d = 30\%$) (Fig. 18b) and completely damped structure ($\xi_d = 100\%$) (Fig. 18c).

It can be seen that the structure in Fig. 18a has an elastic force displacement relationship; therefore, its behaviour is comparable to a simply diagonal brace. One could observe that while the peak force occurs at different displacements it is within 20% higher compared to the partially damped structure (Fig. 18b) and 40% to completely damped (Fig. 18c). However, in Fig. 18c, the axial displacement response is 250% less than that of the structure without the added damping, but the peak overall force is much higher. It is also important to note that the peak force, which occurs at the peak velocity, does not occur at the zero displacement position, which is what would be expected from a standard harmonic

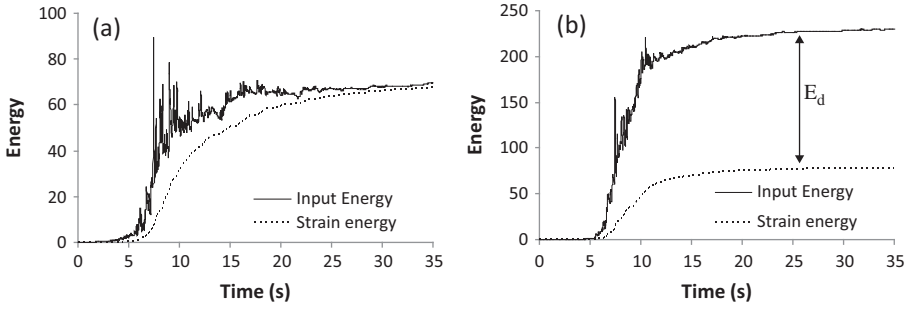

Figure 17 Variation of the input and damping energies of the system without and with FVD.

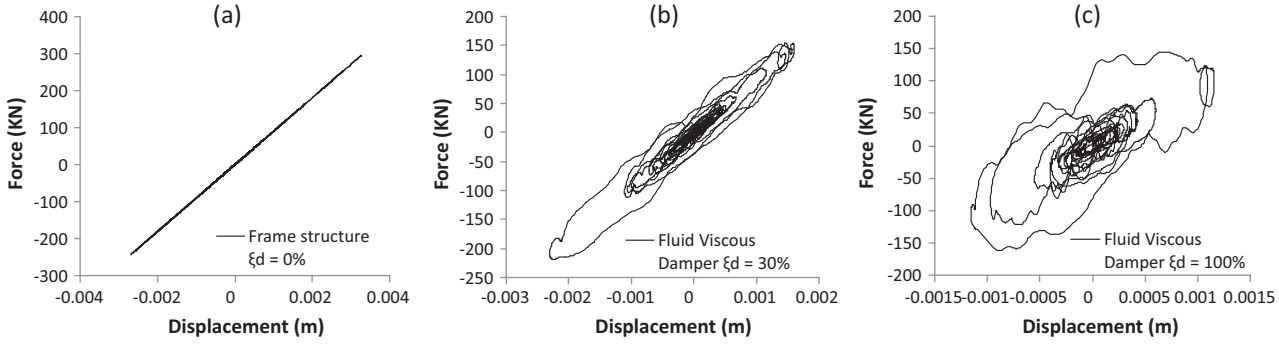

Figure 18 Hysteric loops of damper resistance force versus displacement.

response. This result indicates that the peak velocity induced within the damper, and therefore the peak resistive force imparted into the structure, may be difficult to predict, and higher than expected, despite the simplicity of the structure, model and analysis.

The curves shapes of Fig. 18 are similar to the concept presented schematically in Fig. 5. The results thus highlight the importance of considering the overall balance of damping added, even within realistic ranges of (overall) damping, and especially for cases of structures with augmented damping. Hence, it may be considered that these results justify the overall proof of concept analysis presented in this work.

As expected and as seen above the restoring force induced by the damper generates viscoelastic behaviour which permits greater capacity to dissipate the dynamic loading energies. This plot demonstrates the validity of the analytical model versus to those in the literature review [9].

The analyses of the coefficient of damping C_d distribution at the different stories of the building, have been considered in the curve of Fig. 19. The results showed that the resisting forces generated by the dampers decrease according to the storey height. It means that the damping coefficient used at the upper stories is greater than required for the motion's dissipation. It is induced that the upper dampers are used under the dissipation capacity, in contrast to the lower dampers which are very efficient. The results are in accordance with those in the literature [16,17] which demonstrate that the distribution of its damping ratio must decrease according to the building's height for their more efficient use.

To conclude this study an analysis of relative displacement, relative acceleration and inter-storey drift curves according to the height of building was carried out for the three models. Results are shown respectively in Figs. 20–22.

In general, intrusion of fluid viscous damper in the frame structure results in reduction of the relative floor displacement which varies in a range of 4% in the first storey to 32% at the top storey of the structure (Fig. 20) One may see that the curve representing the variation of the floor acceleration according to the height (Fig. 21) is also flattened. Moreover the comparison of the relative acceleration between the damped and the braced models shows a reduction of 50%. In the other side the difference between the results of damped and undamped is almost minimum despite the increase of stiffness generated by the addition of the dampers.

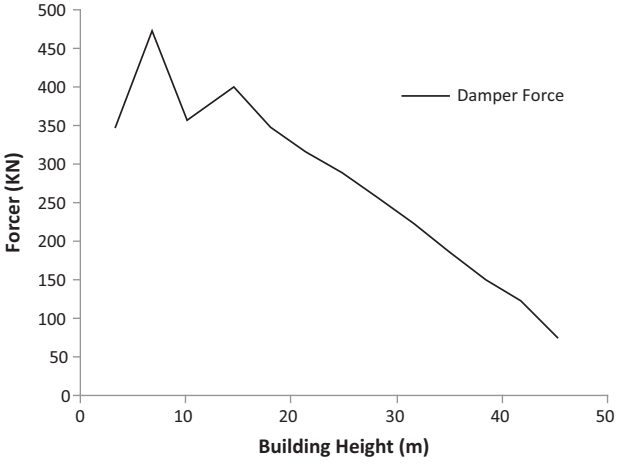

Figure 19 Damping force variation according to building height.

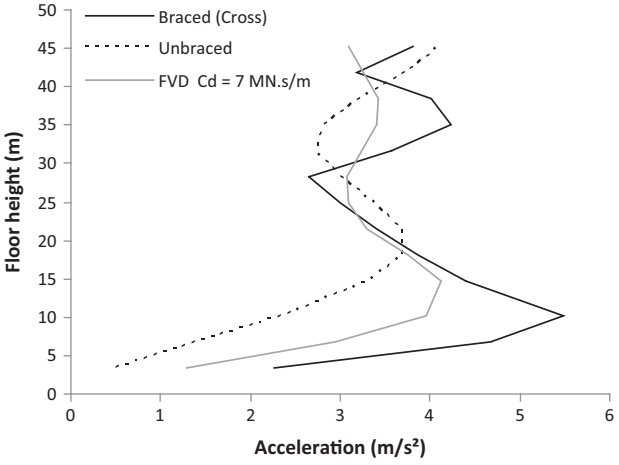

Figure 21 Floor acceleration variations versus building height.

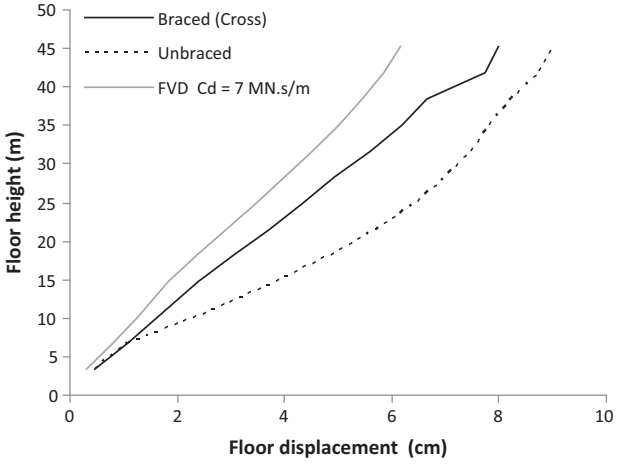

Figure 20 Floor displacement variations versus building height.

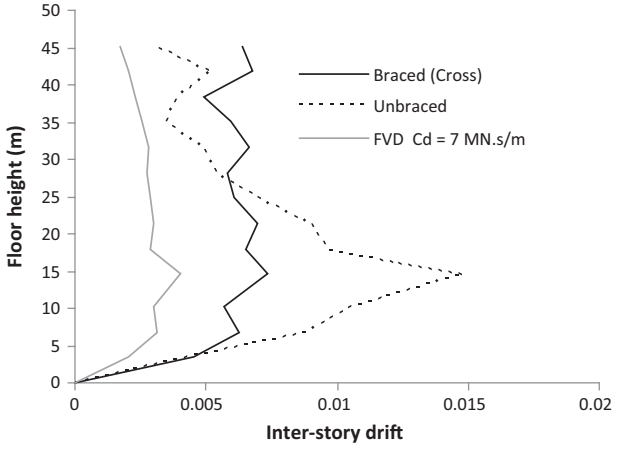

Figure 22 Inter-storey drift variation versus building height.

Finally the analysis of inter-storey drift curve according on the height of building was carried out for the three models. Results are shown in Fig. 22. The variation curve of the damped structure with FVD almost looks like a vertical line whose values are almost constant. The result which is comparable with that achieved by Panah et al. [22], shows that the structure has ones' block behaviour.

4. Conclusions

This study permitted to analyse the difference in steel structure behaviour, with and without viscous damper fluid for a seismic load. Numerical calculation with SAP2000 software was used for the analysis of a 12-storey building. The results show that the use of the passive control device FVD in buildings generates a very significant reduction of the structural response compared to the unbraced ones. However, in the case of a 12-storey building, the main conclusions are summarised below:

- The fundamental period decreases by 220% compared to the unbraced structure.
- The maximum displacements decrease of FVD model until 32% compared to the cross-braced structure.
- Reduction of the maximum acceleration is 37%, which reduces values of base shear forces and its time loading.
- The time history analysis of shear force (V) and bending moment (M) in the most loaded member showed a reduction of these efforts by more than 40%.
- With the damping energy dissipation, the diagonals do not transmit any undesirable axial forces.
- Beyond $C_d = 25$ MN s/m, FVD cannot dissipate supplement seismic energy in the structure.
- The addition of supplemental dampers results an increase of the absolute input energy which is completely dissipated by the increase of damping energy W_D.
- The restoring force induced by the damper generates viscoelastic behaviour which permits greater capacity to dissipate the dynamic loading energies.
- The damping coefficient of the dampers used in structure and/or their number must decrease according to the building height for more efficient use of this device and for economy.
- The difference between the floors' accelerations is minimised.
- The inter-storey drift becomes almost zero, which generates block behaviour of the structure and reduces the effects of shear forces.

The benefits of energy dissipation were clearly demonstrated by the comparison data and improving performance of the structure during an earthquake which has been proved. The passive control system absorbs vibrations automatically and systematically. These devices are generally inexpensive and effective reinforcement of buildings subjected to dynamic excitations.

References

[1] N. Ouali, Effets des Dispositifs D'amortissement sur les Déplacement, Vitesses et Accélérations des Structures, Magister of civil engineering University of Science and technology Houari Boumediene, Algiers, Algeria, 2009

[2] C.M. Uang, V.V. Bertero, Evaluation of seismic energy in structures, Earthq. Eng. Struct. Dynam. 19 (1990) 77–90.

[3] H.K. Miyamoto, A.S. Gilani, S. Wada, State of the art design of steel moment frame buildings with dampers, in: The 14th World Conference of Earthquake Engineering, October 12–17, Beijing, China, 2008.

[4] L.M. Moreschi, Seismic Design of Energy Dissipation Systems for Optimal Structural Performance, Doctor of Philosophy in Engineering Mechanics, Blacksburg, Virginia, US, 2000.

[5] M.G. Oesterle, Use of Incremental Dynamic Analysis to Assess the Performance of Steel Moment-resisting Frames with Fluid Viscous Dampers, Master of Science Thesis, Virginia, USA, 2003.

[6] M.D. Syman, M.C. Constatinou, Passive fluid viscous passive systems for seismic energy dissipation, ISET J. Earthq. Technol. 35 (4) (1998) 185–206, Paper No. 382.

[7] N.S. Armouti, Effect of dampers on seismic demand of short period structures in deep cohesion less sites, Adv. Steel Construct. 7 (2) (2011) 192–205.

[8] J.S. Hwang, Seismic Design of Structures with Viscous Dampers, International Training Programs for Seismic Design of Building Structures Hosted by National Centre for Research on Earthquake Engineering Sponsored by Department of International Programs, National Science Council, January 21–25, Taipei, Taiwan, 2002.

[9] C. Labise, G.W. Rodgers, G.A. MacRae, J.G. Chase, Viscous and hysteretic damping – impact of capacity design violating in augmented structural systems, J. Univ. Canterbury, New Zealand, pp. 23–30, <http://ir.canterbury.ac.nz/handle/10092/7096>.

[10] A. Vulcano, F. Mazza, Comparative study of seismic performance of frames using different dissipative braces, in: 12th World Conference on Earthquake Engineering, Auckland, New Zealand, Sunday 30 January – Friday 4 February, 2000.

[11] N. Markis, M.C. Constatinou, Fractional derivative Maxwell model for viscous damper, J. Struct. Eng. ASCE 117 (9) (1991) 2708–2724.

[12] N. Markis, M.C. Constatinou, Model of viscoelasticity with complex order derivatives, J. Struct. Eng. ASCE 119 (7) (1993) 1453–1464.

[13] M.C. Constantinou, M.D Symans, Experimental and Analytical Investigation of Seismic Response of Structures with Supplemental Fluid Viscous Dampers, Tech Rep. NCEER-92-0027, National Centre for Earthquake Engineering, Research, State Univ. of New York (SUNY) at Buffalo, N.Y., 1992

[14] N. Kaczkowski, Développement des capacités de conception parasismique des ponts, Master of Civil Engineering, Thesis, INSA, Lyon, 2012

[15] FEMA, NEHRP, Guidelines & Commentary for Seismic Rehabilitation of Buildings, Reports N° 273 and 274, October, Washington DC., 1997.

[16] G. Peckman J.B. Mander, S.S. Chen, Design and Retrofit Methodology for Buildings Structure with Supplemental Dissipating Energy Systems, Report N° MCEER 99-002, Multidisciplinary Centre for Earthquake Research, Buffalo, New York, 1999.

[17] K. Bigdeli, Optimal Placement and Design of Passive Damper Connectors for Adjacent Structures, Master of Applied Science Thesis, University of British Columbia, Canada, 2012.

[18] Nonlinear Analysis and Design of Building, SAP2000 User Manual, Computer and Structure, Inc., California, Berkeley, 2002.

[19] RPA99/2003 Algerian seismic code, technical paper DTR B. C 2 48, Algiers, Algeria, 2003.

[20] B. Boukhari, O. Benguedih, Analyse des capacités dissipatives des système de contreventement des structures métallique,

Master thesis of Civil engineering, University Aboubekr Belkaid, Tlemcen, Algeria, 2012.

[21] Y.Y. Lin, C.Y. Chen, Shaking table study on displacement-based design for seismic retrofit of existing buildings using nonlinear viscous damper, in: The 14th World Conference on Earthquake Engineering, Beijing, China, October 12–17, 2008.

[22] E. Yazdan Panah, J. Noorzaei, M.S. Jaafar, M. Seifi, Earthquake response of steel building with viscous brace damper, in: International Conference on Constructing Building Technology, ICCBT2008, 16–20 June 2008 Kuala Lumpur, Malaysia, 2008.